RSC Advances




ROYAL SOCIETY OF CHEMISTRY

www.rsc.org/advances

# MWCNT-CTAB modified glassy carbon electrode as a sensor for the determination of paracetamol

Jayant I. Gowda, Danavva G. Gunjiganvi, Nagaveni B. Sunagar, Manjushree N. Bhat

and Sharanappa T. Nandibewoor*

*P.G. Department of Studies in Chemistry, Karnatak University, Dharwad-580 003, India.*

*Corresponding author: Tel.: +91 836 2215286; Fax: +91 836 2747884

E-mail : stnandibewoor@yahoo.com;

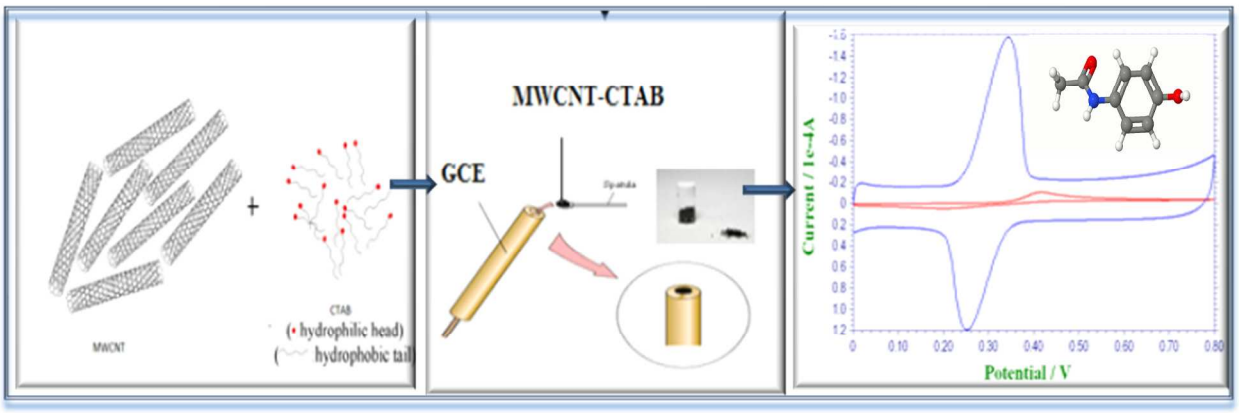

# MWCNT-CTAB modified glassy carbon electrode as a sensor for the determination of paracetamol

Jayant I. Gowda, Danavva G. Gunjiganvi, Nagaveni B. Sunagar, Manjushree N. Bhat

and Sharanappa T. Nandibewoor*

*P.G. Department of Studies in Chemistry, Karnatak University, Dharwad-580 003, India.*

*Corresponding author: Tel.: +91 836 2215286; Fax: +91 836 2747884

E-mail : stnandibewoor@yahoo.com;

**Abstract**

An electrochemical sensor for sensitive detection of paracetamol (PCM) was developed by constructing the glassy carbon electrode (GCE) modified with multiwalled carbon nanotube-cetyltrimethyl ammonium bromide (MWCNT-CTAB). Modification improves the redox kinetics of PCM with increased current intensity. A similar modification at CTAB modified GCE did not result in an impressive charge transfer. Detection limit of PCM was determined from differential pulse voltammetric (DPV) study and found to be $4.82\times10^{-9}$ M with a linear dynamic range of $4.0\times10^{-7}$ M to $4.0\times10^{-6}$ M. The interference studies showed that the modified electrode exhibits excellent selectivity in the presence of large excess of interferents and response is fast, stable, reliable, resistant to biofouling and can be applied for the real sample analysis in medical, pharmaceutical and biotechnological sectors. Kinetic parameters were determined using electrochemical approaches. The practical analytical application of this electrode was demonstrated by measurement of PCM content in PYREMOL 650 tablet and real sample analysis.

**Keywords:** Voltammetry, Modified electrode, Paracetamol, Electro-oxidation, Pharmaceutical analysis

## 1. Introduction

Sensors based on multi-walled carbon nanotubes (MWCNTs) were widely used in various electrochemical applications in the last years, since they display numerous advantages, such as great electrochemically accessible area, high electrical conductivity, extremely high reactivity and selectivity, as well as great chemical stability[1]. Furthermore, it was recognized that MWCNTs exhibit improved electric transport properties and electrocatalytic properties and are capable to reduce the over potentials and to improve significantly the currents of redox systems[2-4]. In addition, MWCNTs display high sensitivity and detection capability, and thus, they improve the reaction rate and amplify the stability and reproducibility of electrode's response[5]. Cetyltrimethylammonium bromide (CTAB), a cationic surfactant, often used as an absorbent due to the strong hydrophobic interaction between the long alkyl chain of CTAB. In this case, CTAB can be used as electrode modifier for enrichment of MWCNTs on the electrode surface to improve sensitivity.

Paracetamol (N-acetyl-p-aminophenol or acetaminophen, PCM) is the most widely used antipyretic and analgesic drug in the world[6]. It is not only an effective and safe analgesic agent used for the relief of mild to moderate pain associated with headache, arthritis, backache, toothaches and postoperative pain, but also used for reduction of fevers of viral and bacterial origin[7,8]. Generally, paracetamol does not exhibit any harmful side effects. However, abnormal level of paracetamol is believed to be associated with the formation of some liver and nephrotoxic metabolites[9,10]. In addition, the use of acetaminophen in children younger than one year may cause an increase in hinoconjunctivitis, asthma, and eczema[11]. Therefore, determination of PCM in biological samples and quality control in pharmaceuticals is very important considering the enormous interest of PCM for therapeutic purposes.

Many analytical methodologies based on different principles, such as titrimetry[12], spectrophotometry[13], chromatography[14], capillary electrophoresis[15], chemiluminescence[16] and flow-injection analysis[17] have been developed for the analysis of PCM. However, these methods require expensive instruments, long analysis time, highly skilled technician and laborious sample pretreatment, which make them unsuitable for routine analysis. Taking the above mentioned lacune and the high electroactivity of PCM into consideration, electrochemical analytical techniques for PCM determination has been

widely explored method due to simplicity, high sensitivity, low cost, easy operation and possibility to miniaturization[18-21]. However, at traditional working electrodes, PCM exhibit poor voltammetric response due to sluggish electrode kinetics[22]. Another problem commonly encountered at bare electrode is that they get poisoned by several species and decrease sensitivity and reproducibility. Hence, considerable efforts have been devoted to modify the electrode for enhancing its voltammetric response and analytical performance [23-36]. In the present work, the dispersion of multiwalled carbon nanotubes in the presence of CTAB surfactant modified glassy carbon electrode was used as suitable sensor for the determination of PCM. The proposed method was applied to pharmaceutical sample and real samples.

## 2. Materials and methods

### *2.1. Reagents and chemicals*

Paracetamol was purchased from s.d. fine Chem limited and multi walled carbon nanotubes (MWCNTs) powders was purchased from Sigma Aldrich. Cetyltrimethylammonium bromide was from Merck. A solution of paracetamol was prepared by dissolving an appropriate amount of powdered sample in double distilled water. Double distilled water was used throughout the work. All other solvents and materials used were of analytical grade.

### *2.2. Instrumentation and analytical procedure*

The electrochemical experiments were performed with a CHI630D Electrochemical analyzer with a three electrode system. A MWCNT-CTAB/GCE serves as the working electrode, a platinum wire as the auxiliary electrode, and an Ag/AgCl (3.0 MKCl) as the reference electrode, respectively. pH measurements were performed with Elico LI120 pH meter (Elico Ltd., India). Experiments were carried out at room temperature.

The parameters for differential pulse voltammetry (DPV) were initial potential: 0.4V; final potential: 1.4; increase potential: 0.004 V; amplitude: 0.05 V; frequency: 15 Hz; with time: 2 s; sensitivity:$1\times10^{-4}$ A\V.

### *2.3. Preparation of modified electrode*

To get reproducible results, great care was taken in the electrode pre-treatment. The GCE was pre-treated in two ways: (i) mechanical polishing over a velvet micro-cloth with 0.3 and 0.05 m alumina slurry and (ii) electrochemical treatment by applying a potential of 1.25 V for 2 s. The electrochemical pre-treatment was done in the same supporting electrolyte solution in

which the measurement was carried out. Solution containing 0.3 g/L MWCNTs and 0.2 g/L CTAB was sonicated for 60 min. 10 µL of the sonicated solution was placed on the GCE surface and then evaporating in an oven at 50 °C. The ultrasonication of MWCNTs via CTAB will lead to the dispersion of nanotubes, and fix the surfactants on the surface of MWCNTs (Possible arrangements of CTAB on MWCNTs are illustrated in Supplementary Fig. S1[37]. It is described that the cationic surfactant make the nanotubes positively charged; these charged MWCNTs are driven toward cathode to form a thin layer at the electrode surface.

Eventually, the coated electrodes (MWCNTs-CTAB/GCE) were immersed in the bicarbonate solution (0.01 M) for 30 min in order to extract the residual surfactants from the surface of electrode. The modified electrodes were washed with distilled water and dried in room temperature (MWCNTs–GCE). Fig. 1 shows surface morphology of photography AFM images of MWCNT and MWCNT-CTAB.

**"Here Figure 1"**

*2.4. Pharmaceutical sample preparation*

Three tablets of containing paracetamol were weighed, powdered and then placed into a 250 ml of conical flask; warm water was added into the flask. The sample was swirled to dissolve for 30 minutes in sonicator and left cool. The sample solution was filtered through a filter paper (Whatman No.42) into 100 ml volumetric flask. The filtrate was make up to the volume with 0.2 M phosphate buffer pH 7.4 for the direct calibration method and standard addition method, respectively.

*2.5. Plasma sample preparation*

Human plasma sample was prepared as described in the earlier report of our work[38]. Human blood samples were collected in dry and evacuated tubes (which contained saline and sodium citrate solution) from a healthy volunteer. The samples were handled at room temperature and were centrifuged for 10 min at 1500 rpm for the separation of plasma within 1 h of collection. The samples were then transferred to polypropylene tubes and stored at -20 °C until analysis. The plasma samples, 0.2 mL, were deprotonised with 2 mL of methanol. After vortexing for 15 min, the mixture was then centrifuged for 15 min at 6000 rpm, and supernatants were collected.

**3. Results and discussion**

*3.1. Electrocatalytic response of PCM at the MWCNT-CTAB modified glassy carbon electrode*

Cyclic voltammetry was used to investigate the electrochemical behavior of paracetamol on a MWCNT-CTAB/GCE in the phosphate buffer solution (0.2 M, pH 7.4) at a scan rate of 50 mV $s^{-1}$. It can be seen that paracetamol shows a quasi-reversible redox behavior with relatively weak redox peaks at the bare GCE, which indicates that the direct electron transfer of paracetamol at the bare GCE is very slow. The redox peak currents are higher than that at the bare GCE with $I_{pa}/I_{pc} \approx 1$. The redox performs a quasi-reversible process because the nanocomposite film of MWCNT-CTAB can accelerate the electrochemical reaction. It can be seen from Fig. 2. that there is a large background current at the MWCNT-CTAB modified GCE, which is caused by a larger surface area of the nanocomposite film on the GCE.

**"Here Figure 2"**

*3.2. Effect of amount of MWCNT-CTAB suspension*

We examined the effect of MWCNT-CTAB suspension amount on the electrochemical behavior of PCM. The results suggested that amount of MWCNT-CTAB suspension influenced the current responses of PCM. Supplementary Fig. S2 demonstrates the relationship between the oxidation peak current of PCM and the amount of MWCNT-CTAB suspension used for coating GC electrode. As can be seen, the peak current gradually increased with increasing the amount of MWCNT-CTAB suspension from 0 to 10 μL, owing to the increased effective electrode surface area for PCM oxidation. Further increasing the amount of MWCNT-CTAB suspension, the peak current almost remained stable. However, when it exceeded 14 μL, the peak current slightly decreased. When the coating film was too thick, the film no longer adhered tightly to the glass carbon, reducing conductivity and part of the MWCNT-CTAB left the electrode surface. More excessively coated amount of MWCNT-CTAB suspension led to less adherent film. Accordingly, 10 μL of MWCNT-CTAB suspension solution providing the maximum current response was used in further experiments, while the amount of suspension of MWCNT-CTAB had little effect on the oxidation potential of PCM.

*3.3. Effect of pH*

The electrochemical response of PCM at MWCNT-CTAB/GCE was generally dependent on pH. The voltammograms of PCM were recorded at 0.2 M phosphate buffer solution of different pH by cyclic voltammetric method. Fig. 3(a) demonstrates the pH dependence of PCM at MWCNT-CTAB/GCE at sweep rate of 50 mV $s^{-1}$. Both anodic and cathodic peak potentials were shifted to less positive side with increasing in the pH values. The anodic peak potential of

PCM shifted from 0.547 to 0.238 mV with increase in the pH 3.0 –11.2. The potential diagram was constructed by plotting the graph of $E_{pa}$ vs. pH of the solution (Fig. 3(b)). The graph shows good linearity with a slope of 51 mV/pH this behavior is nearly obeyed the Nernst equation for equal number of electron and proton transfer reaction[39, 40]. From the graph of $I_{pa}$ vs. pH, maximum current was obtained at pH 7.4 (Fig. 3(c)) and for further studies pH 7.4 was selected for PCM determination.

**"Here Figure 3 (a), 3(b), 3(c)"**

*3.4. Effect scan rate*

The effect of scan rate on the electro-oxidation of PCM at the MWCNT-CTAB/GCE was investigated by cyclic voltammetry to acquire information about electrochemical mechanism from the relationship between peak current and scan rate of potential. The cyclic voltammograms of 0.1 mM PCM at MWCNT-CTAB/GCE (Fig. 4(a)) were recorded at different scan rates from 0.025 to 0.4 V $s^{-1}$, as well. The anodic ($I_{pa}$) and cathodic ($I_{pc}$) peak currents are found to be linearly dependent on *v* at scan rates of 0.025 to 0.4 V $s^{-1}$. A linear correlation is obtained between the peak current and the scan rate, indicating that the redox process is controlled by adsorption. The regression equations are $I_{pa}(10^{-4}A) = 1.764 + 55.401v$ (V $s^{-1}$); $R^2 = 0.991$ and $I_{pc}(10^{-4}A) = 1.306 + 36.88$ v (V $s^{-1}$); $R^2 = 0.993$ (Fig. 4(b)). From the plot of log $I_p$ vs log scan rate the slope values are nearly equal to the 0.5 of purely diffusion controlled process. Hence the process is diffusion controlled (Supplementary Fig. S3).

The anodic and cathodic peak potentials are found to be linearly dependent on log *v* at scan rates of 0.025 to 0.40 V $s^{-1}$ (Fig. 4(c)). Two straight lines were obtained with two linear regression equations as $E_{pa}(V) = 0.087 \log v + 0.384$; $R^2 = 0.9916$ and $E_{pc}(V) = -0.089 \log v + 0.180$; $R^2 = 0.9918$. Under these conditions, the $k_s$ can be obtained according to the following equations[41];

$$E_{pa} = E^{0'} + \left(\frac{2.303RT}{(1-\alpha nF)}\right)\log v + \left(\frac{2.303RT}{(1-\alpha nF)}\right)\log\left(\frac{nF(1-\alpha)}{RTk_s}\right) \qquad (1)$$

$$E_{pc} = E^{0'} - \left(\frac{2.303RT}{(\alpha nF)}\right)\log v - \left(\frac{2.303RT}{(\alpha nF)}\right)\log\left(\frac{\alpha nF}{RTk_s}\right) \qquad (2)$$

$$\log k_s = \alpha\log(1-\alpha) + (1-\alpha)\log\alpha - \log\frac{RT}{nFv} - \frac{\alpha(1-\alpha)nF\Delta E_p}{2.3RT} \qquad (3)$$

According to the slopes of two curves ($E_{pa}$ vs. log v and $E_{pc}$ vs. log v) and Eq. (1) and Eq. (2), α was calculated to be 0.51 and number of electrons (n) was 1.92 ≈ 2.0. With the Eq. (3), a value of $k_s = 2.397 \times 10^{-5}\ s^{-1}$ was obtained from all the extracted experimental data.

**"Here Figure 4(a), 4(b), 4(c)"**

*3.5. Mechanism*

UV spectrum of 0.1 mM PCM in 0.2 M phosphate buffer solution in pH 7.4 before and after electrolysis are shown in Fig. 5. One absorption peak was found at 243.5 nm before electrolysis (curve a). The electrolysis was carried out for 6 h. After depleting electrolysis, the absorption peak at 243.5 nm slightly vanishes (curve b). We speculate that electro oxidation might have lead to destruction of the pi bond conjugate system in PCM. This was also supported by the earlier report[42]. The number of electrons and hydrogen ions transferred was 2. With all the previous experimental results, a possible electrode reaction mechanism for PCM might be expressed as shown in Scheme 1.

**"Here Figure 5"**

**"Here Scheme 1"**

*3.6. Analytical performance*

*3.6.1. Linearity range and detection limit using voltammetry*

Under the optimized experimental conditions, the quantitative analysis of PCM was carried out by the fabricated sensor. Since a large capacitive current existed in CV measurements, the differential pulse voltammetry (DPV) was applied in this assay because its charging current contribution to the background current is quite low. Fig. 6(a) shows the dependence of the DPV oxidation peaks on the concentrations of PCM. It is found that with the

increase of the PCM concentrations, the DPV oxidation signals enhance gradually, and an excellent linearity is observed over a wide concentration range from $4.0 \times 10^{-7}$ M to $4.0 \times 10^{-6}$M, $I_{pa}$ ($10^{-4}$A) = 2.47 [PCM](μM) + 6.534 ($R^2$=0.9894) (Fig. 6(b)). Based on the signal-to-noise ratio (S/N) of 3, the detection limit was estimated to be $4.82 \times 10^{-9}$ M and limit of quantification was $1.60 \times 10^{-8}$ M as shown in Table 1. Referring to the analytical performances of some recently published reports[43-58](Table 2), it is found that the obtained detection limit in this work is lower than other modified electrodes, which is likely related that MWCNT-CTAB have high electrocatalytic and surface area effects. But, compared with the electrode modified with the other materials like SWCNTs, MWCNTs, CPB/CNTP and $C_{60}$, our developed method shows the lower detection limit and the wider kinetic range, suggesting that the developed sensor in this work can be served as a promising platform for the sensitive detection of PCM in low concentration.

**"Here Figure 6(a) 6(b)"**

**"Here Table 1"**

**"Here Table 2"**

Additionally, a relative standard deviation of 2.5% for $1.0 \times 10^{-3}$ M PCM (n=5) suggests that the MWCNT-CTAB/GCE modified electrode has good reproducibility. Six electrodes fabricated independently were used to determine $1.0 \times 10^{-4}$ M PCM, and the relative standard deviation is 3.0%, revealing an excellent repeatability of the electrode preparation. The stability of the film electrode was evaluated by measuring the peak current of $1.0 \times 10^{-4}$M PCM repeatedly. It is found that after 40-times test, the peak current deviates from its original response only 5%.

*3.6.2. Linearity range and detection limit using UV data*

The working standard solutions for the drug PCM having concentration 2 to 150 μM were prepared with phosphate buffer 7.4 from the stock solution. The linearity was determined by plotting standard calibration curves for the concentration range 2-150 μM at 248 nm as shown in Fig. 7(a,b). The limit of detection (LOD) and limit of quantifications (LOQ) of paracetamol were evaluated from the slope (m) of their respective calibration curve and the standard deviation of the blank (s) using equations as:

$$LOD = 3s/m; LOQ = 10\ s/m$$

Using the detection limit was estimated to be $3.39 \times 10^{-6}$ M and limit of quantification was $1.13 \times 10^{-5}$ M as shown in Table 1. Comparing the LOD values obtained by means of spectroscopic and voltammetric technique, we achieved a lower detection limit for PCM by voltammetric technique.

**"Here Figure 7(a) 7(b)"**

*3.7. Determination of PCM in pharmaceutical preparations and recovery test*

The proposed method was validated for the determination of PCM in pharmaceutical preparations in "PYREMOL 650" tablets (650 mg per tablet) as a real sample by applying DPV using the standard addition method. PYREMOL 650 tablets (Shiva Biogenetics Pharmaceuticals Pvt. Ltd., India) labeled as containing 650 mg of PCM per tablet were weighed and ground to a homogeneous fine powder in a mortar. A portion equivalent to a stock solution of a concentration of about 0.01 M was accurately weighed and transferred into a 100 mL calibrated flask and completed to the volume with doubly distilled water. The contents of the flask were sonicated for 15 min to affect complete dissolution. Appropriate solutions were prepared by taking suitable aliquots of the clear supernatant liquor and diluting them with the phosphate buffer solution. Each solution was transferred to the voltammetric cell and analyzed by standard addition method. The differential pulse voltammograms were recorded between 0 and 0.5 V. The oxidation peak current of PCM was measured at scan rate of 50 mV $s^{-1}$. To study the accuracy of the proposed method and to check the interferences from excipients used in the dosage form, recovery experiments were carried out. The concentration of PCM was calculated using the standard addition method. The results are in good agreement with the content marked in the label (Table 3).

**"Here Table 3"**

*3.8. Interference study*

The potential interference for the determination of PCM was also studied. Under the optimized conditions, the oxidation peak of $1.0 \times 10^{-6}$ M PCM was individually measured in the presence of different concentrations of the common interferents, and then the change of peak current was checked. It is found that glucose, citric acid, dextrose, gum acacia, oxalic acid,

starch, tartaric acid almost have no influence on the detection of PCM since the peak current change is below 5%, however gum acacia had apparent influence on the voltammetric signal of PCM(Table 4), revealing that this sensor has good selectivity for PCM determination.

**"Here Table 4"**

*3.9. Application to real matrices*

To evaluate the applicability of the present method on real matrices, assays were performed in serum and urine samples. To ascertain the validity of the results, the real samples were spiked with certain amount of PCM. The results showed that satisfactory recovery for PCM could be obtained (Table 5).

**"Here Table 5"**

## 4. Conclusion

A novel method is described for the determination of paracetamol which is simple, quick and sensitive with a low cost analysis. A comparison of the voltammetric response of paracetamol at bare GCE, MWCNT modified GCE and MWCNT-CTAB modified GCE clearly revealed that MWCNT in presence of CTAB acts as a better surface modifier in comparison to MWCNT at fixed concentration of nanotubes in mg/mL of the solvent. Such a deposition imparts different effective surface areas to electrodes. The sensitivity at MWCNT-CTAB modified GCE was found to be ~1.5 times more in comparison to MWCNT modified GCE with a lower detection limit. The quantitative evaluation of the compound was carried out in the range of 0.4–4.0 μM with a detection limit of $4.92\times10^{-9}$ M at MWCNT-CTAB modified GCE. To the best of our knowledge, this limit of detection is the lowest value reported for paracetamol using electrochemical techniques. The MWCNT-CTAB modified GCE exhibited a stable and reproducible response for paracetamol determination without any influence of physiologically common interferents. The usefulness of the method was demonstrated by applying it to the analysis of pharmaceutical preparations and human urine and plasma samples. Thus, the proposed method using differential pulse voltammetry is of beneficial use in analytical applications and in fundamental studies of electrode mechanisms.

**References**


1. S. Ranganathan, T. Kuo and R.L. McCreery, *Anal. Chem.*, 1999, **71,** 3574-3580.
2. B. S. Sherigara, W. Kutner and F. D'Souza, *Electroanalysis*, 2003, **15,**753-772.
3. L.Y. Matzui, I. V.Ovsienko, T.A. Len, Y. I. Prylutskyy, P. Scharff, Fuller Nanotubes *Carbon Nanostruct*., 2005, **13,** 259-261.
4. V. Ovsienko, T.A. Len, L.Y. Matzui, Y.I. Prylutskyy, U. Ritter, P. Scharff, F. Le Normand and P. Eklund, *Mol. Cryst. Liq. Cryst.*, 2007, **468,** 289-297.
5. Y.H. Yun, Z. Dong, V. Shanov, W.R. Heineman, H.B. Halsall, A. Bhattacharya, L. Conforti, R.K. Narayan, W.S. Ball and M.J. Schulz, *Nano Today*, 2007, **2,** 30-38.
6. Martindale, The Extra Pharmacopoeia, 29th ed., The Pharmaceutical Press, London, 1989, pp. 32.
7. L. Jia, X.H. Zhang, Q. Li and S.F. Wang, *J. Anal. Chem*. 2007, **62,** 266-269.
8. R.T. Kachoosangi, G.G. Wildgoose and R.G. Compton, *Anal. Chimica Acta*, 2008, **618** 54-60.
9. D.W. Cramer, B.L. Harlow, L. Titus-Ernstoff, K. Bohlke, W.R. Welch and E.R. Greenberg, *The Lancet,*1998*,* **351,** 104-107.
10. A.K. Rowden, J. Norvell, D.L. Eldridge and M.A. Kirk, *Clinics Lab. Med*. 2006, **26,** 49-65.
11. J.E. Sullivan and H.C. Farrar, *Pediatrics,*2011, **127,** 580-587.
12. G. Burgot, F. Auffret and J.L. Burgot, *Anal. Chim. Acta,*1997*,* **343,**125-128.
13. Sirajuddin, A.R. Khaskheli, A. Shah, M.I. Bhanger, A. Niaz and S. Mahesar,
    a. *Spectrochim. Acta A,* 2007, **68,** 747-751.
14. A. Goyal and S. Jain, *Acta Pharm. Sciencia*, 2007, **49,** 147-151.
15. M. E. Capella-Peiró, D. Bose, M.F. Rubert and J. Esteve-Romero, *J. Chromatography B.,* 2006, **839,** 95-101.
16. D. Easwaramoorthy, Y.C. Yu and H.J. Huang, Anal. Chimica Acta, 2001, **439,** 95-100.
17. M. Knochen, J. Giglio and B.F. Reis, *J. Pharm. Biomed. Anal.*, 2003, **33,** 191-197.
18. A.A. Ensafi, H. Karimi-Maleh, S. Mallakpour and M. Hatami, *Sens. Actuators B,*2011, **155,** 464-472.

19. N.F. Atta, A. Galal, F.M. Abu-Attia and S.M. Azab, J. Mat. Chem.,2011,**21,** 13015-13025.
20. M.P.N. Bui, C.A. Li, K.N. Han, X.H. Pham and G.H. Seong, *Sens. Actuators B*. 2012, **174,** 318-324.
21. X. Chen, J. Zhu, Q. Xi and W. Yang, *Sens. Actuators B,* 2012, **161,** 648-654.
22. A. Safavi, N. Maleki and O. Moradlou, *Electroanalysis*, 2008, **20**, 2158-2162.
23. Y.Fan , J. H. Liu, H. T. Lu and Q. Zhang , *Coll. Sur*. B, 2011, **85**, 289–292.
24. H.Gorcay, G. Turkoglu, Y. and H. Berber, *Sensors Journal*, 2014, **14**, 2529 - 2536.
25. C. X. Xu , K. J. Huang, Y. Fan, Z. W. Wu and J. Li, *J. Mol. Liq*., 2012, **165**, 32-37.
26. Y. Fan, J. H. Liu , H. T. Lu and Q. Zhang, *Coll. Surface B*, 2011, **85**, 289-892.
27. K. S. Ngai, W. T. Tan, Z. Zainal, R. M. Zawawi and J. C. Juan, *Adv. Mat. Sci. Eng*., 2015, **2015**, 1-8.
28. D. Sun and H. Zhang , *Microchimica Acta* , 2007, **158**, 131-136.
29. M. Behpour, S. M. Ghoreishi, M. Meshki and H. Naemi, *J. Anal. Chem*. 2014, **69**, 982-989.
30. Kalimuthu, P. John and S. Abraham, *Electroanalysis*, 2010, **22**, 303-309.
31. H. Yin, X. Meng, Z. Xu, L. Chen and S. Ai, *Anal. Methods*, 2012, **4**, 1445-145.
32. N. F. Atta, A. Galal and S. M. Azab, *Int. J. Electrochem. Sci*., 2011, **6**, 5082 - 5096.
33. H. Filik, G. Çetintaş, A. A. Avan, S. N. Koç and İ. Boz, *Int. J. Electrochem. Sci*., 2013, **8**, 5724 - 5737.
34. M. Zidan, R. M. Zawawi, M. Erhaye and A. Salhin, *Int. J. Electrochem. Sci*., 2014, **9**, 7605 - 7613.
35. X. Kang, J. Wang, H. Wu, J. Liu, I. A. Aksay and Y. Lin, *Talanta*, 2010, **81**, 754–759.
36. K. J. Gururaj, B. E. Kumara Swamy *Soft Nanoscience Letters*, 2013, 3, 20-22.
37. E. Pajootan and M. Arami, *Electrochim. Acta*, 2013, **112,**505-513.
38. J. I. Gowda and S. T. Nandibewoor, *Ind. Eng. Chem. Res*. 2012, **51**,15936−15941.
39. H. Yao, Y. Sun, X. Lin, Y. Tang, A. Liu, G. Li, W. Li and S. Zhang, *Anal. Sci*. 2007, **23**, 677-682.
40. B.D. Jones and J.D. Ingle Jr., *Talanta*, 2001, **55,** 699-714.

41. Z. Wang, J. Xia, L. Zhu, X. Chen, F. Zhang, S. Yao, Y. Li and Y. Xia, *Electroanalysis* **,** 201**0, 22,** 7-19.
42. Y.H. Zhu, Z.L. Zhang and D.W. Pang, *J. Electroanal. Chem*. 2005, **581,** 303-309.
43. B. Habibi and M. Jahanbakhshi, M.H. Pournaghi-Azar, Anal. Biochem. 2011**,411,** 167-175.
44. X. Chen, J. Zhu, Q. Xi and W. Yang, *Sen. Actuators B*., 2012*,* **161,** 648-654.
45. A. Babaei, M. Afrasiabi, S. Mirzakhani and A. Reza Taheri, *J. Braz. Chem. Soc*. 2011, **22,** 344-351.
46. J.B. Raoof, R. Ojani, M. Baghayeri and M. Amiri-Aref, *Anal. Methods*, 2012, **4,** 1579-1587.
47. Y. Umasankar, B. Unnikrishnan, S.M. Chen and T.W. Ting, *Int. J. Electrochem. Sci*. 2012, **7,** 484-498.
48. P.R. Dalmasso, M.L. Pedano and G.A. Rivas, *Sens. Actuators B*., 2012**,173,**732-736.
49. A. Babaei, D.J. Garrett and A.J. Downard, *Electroanalysis,* 2011, **23,** 417-423.
50. R. Manjunatha, D.H. Nagaraju, G.S. Suresh, J.S. Melo, S.F. D'Souza and T.V. Venkatesha, *Electrochim. Acta,* 2011, **56,** 6619-6627.
51. A.A. Ensafi, H. Karimi-Maleh, S. Mallakpour and M. Hatami, *Sens. Actuators B*., 2011, **155**, 464-472.
52. M. Asnaashariisfahani, H. Karimi-Maleh, H. Ahmar, A. A. Ensafi, A.R. Fakhari, M.A. Khalilzadeh and F. Karimi, *Anal. Methods*, 2012, **4,** 3275-3282.
53. M. Keyvanfard, R. Shakeri, H. Karimi-Maleh and K. Alizad, *Mat. Sci. Eng. C.*, 2013, **33,** 811-816.
54. E.H. Duarte, L.T. Kubota and C.R.T. Tarley, *Electroanalysis*, 2012, **24,** 2291-2301.
55. C. Radovan, C. Cofan and D. Cinghita, *Electroanalysis*, 2008*,* **20,** 1346-1353.
56. N. Havens, P. Trihn, D. Kim, M. Luna, A.K. Wanekaya and A. Mugweru, *Electrochim. Acta,* 2010, **55,** 2186-2190.
57. S. F. Wang, F. Xie and R.-F. Hu, *Sens. Actuators B*, 2007, **123,** 495-500.
58. J. M. Zen and Y. S. Ting, *Anal. Chim. Acta*, 1997, **342,** 175-180.

**Fig. 1.** AFM topography of (A) MWCNTs, (B) MWCNT-CTAB sample

(A). AFM image of GCE surface modified with MWCNTs

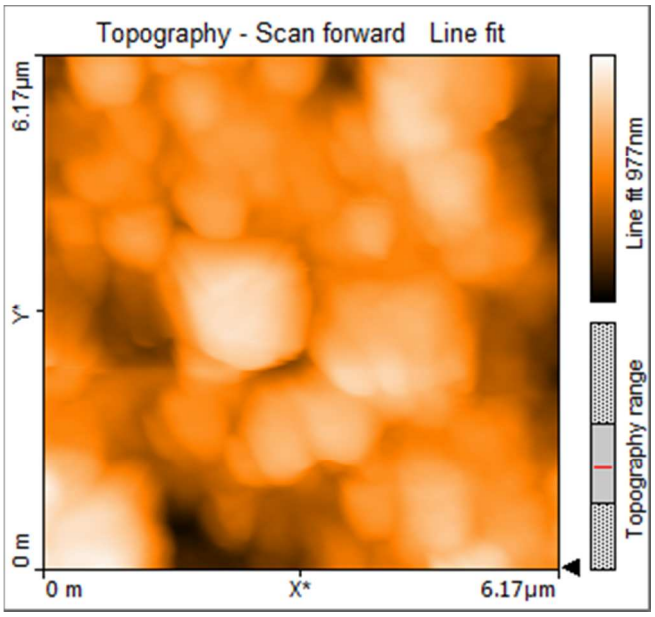


(B). AFM image of GCE surface modified with MWCNT-CTAB

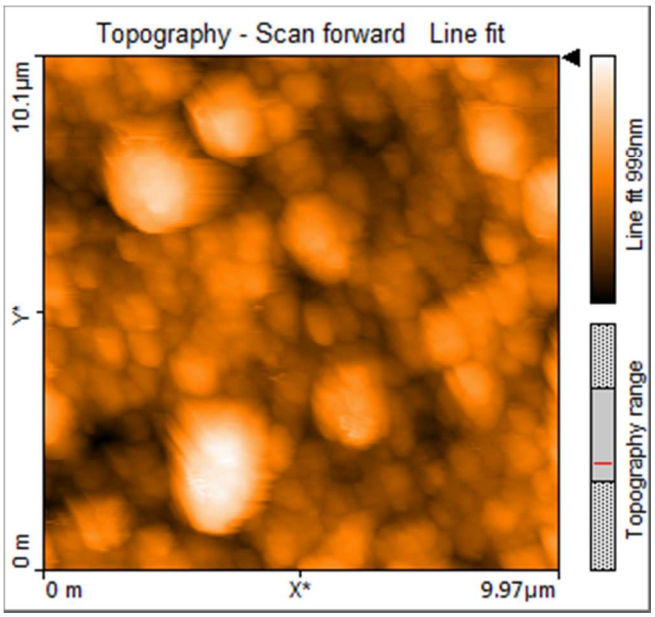

**Fig. 2**. Cyclic voltammograms obtained for 0.1 mM paracetamol at pH 7.4 at (a) bare GCE, (b) MWCNT modified GCE and (C) MWCNT-CTAB modified GCE at 50 mV $s^{-1}$.

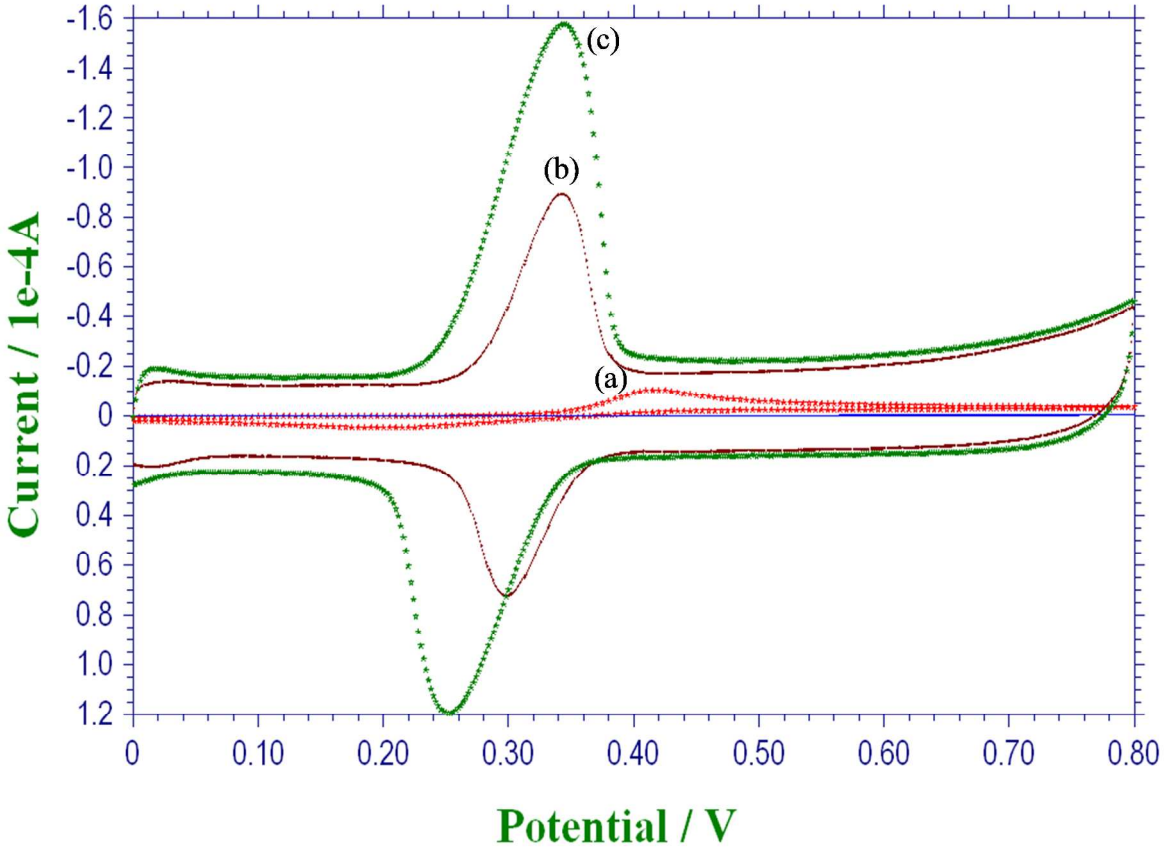

**Fig. 3(a).** Influence of pH (a-i : 3.0-11.2) on the shape of anodic peak of 1.0 $\times 10^{-4}$ M PCM on MWCNT-CTAB/GCE at scan rate of 50 mV $s^{-1}$ in phosphate buffer.

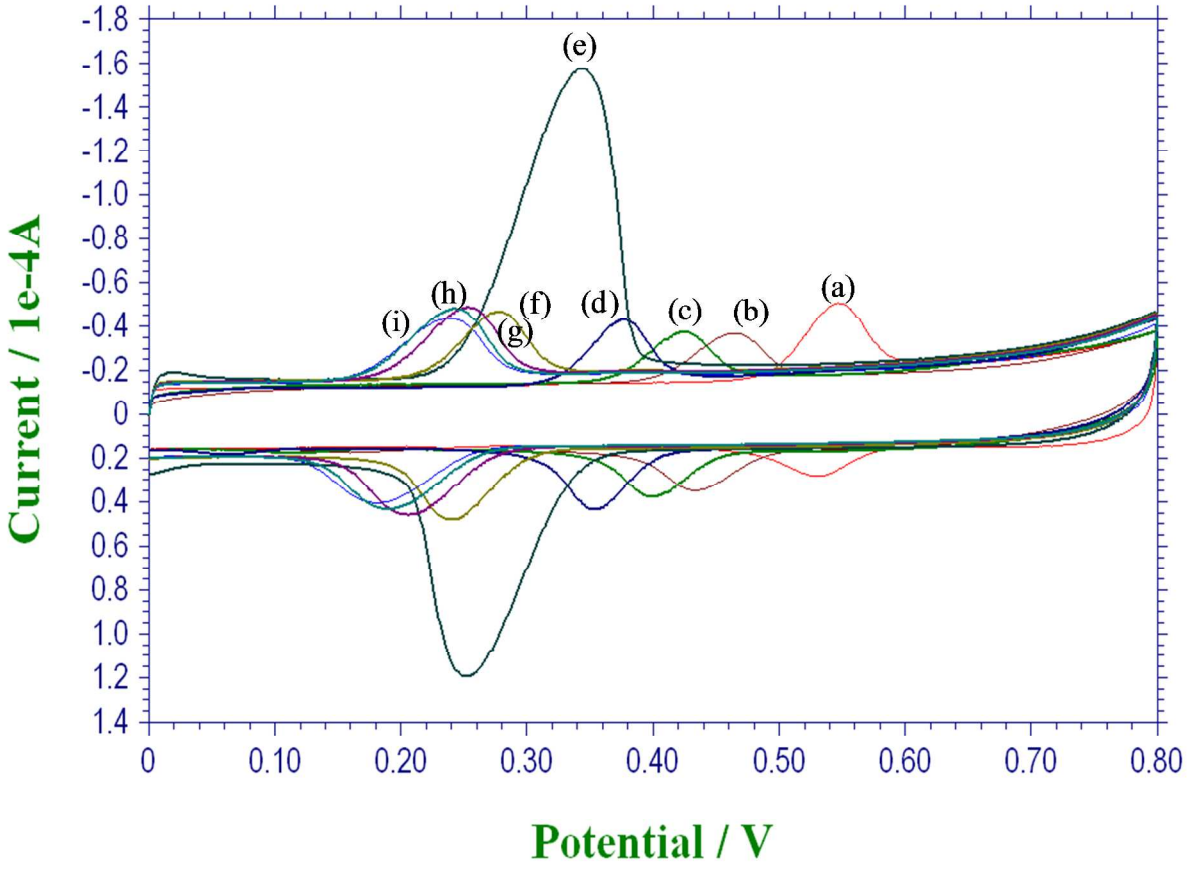

**Fig. 3(b).** Influence of pH on the potential of $1.0\times10^{-4}$ M PCM on MWCNT-CTAB/GCE at scan rate of 50 mV $s^{-1}$ in phosphate buffer.

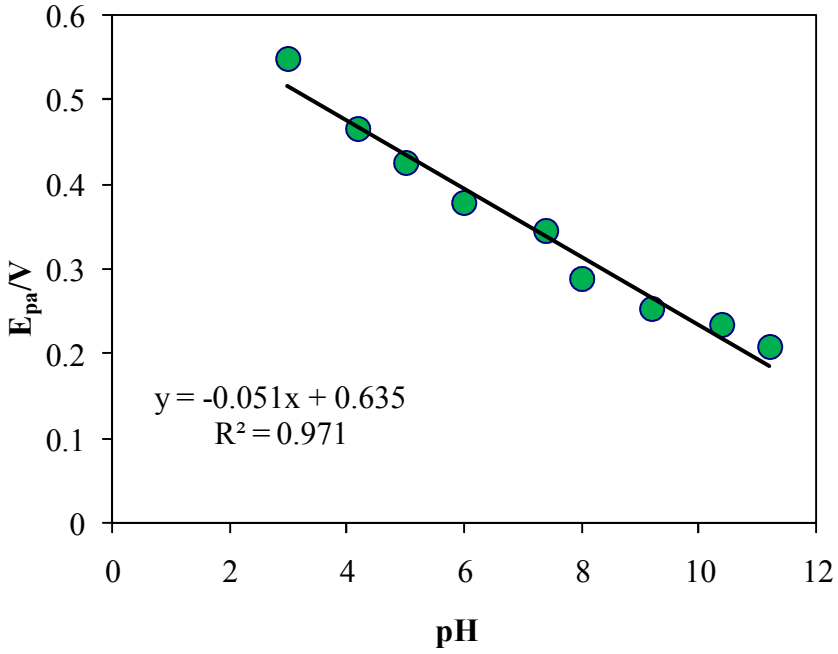


**Fig. 3(c).** Variation of current with pH of $1.0\times10^{-4}$M PCM on MWCNT-CTAB/GCE at scan rate of 50 mV $s^{-1}$ in phosphate buffer.

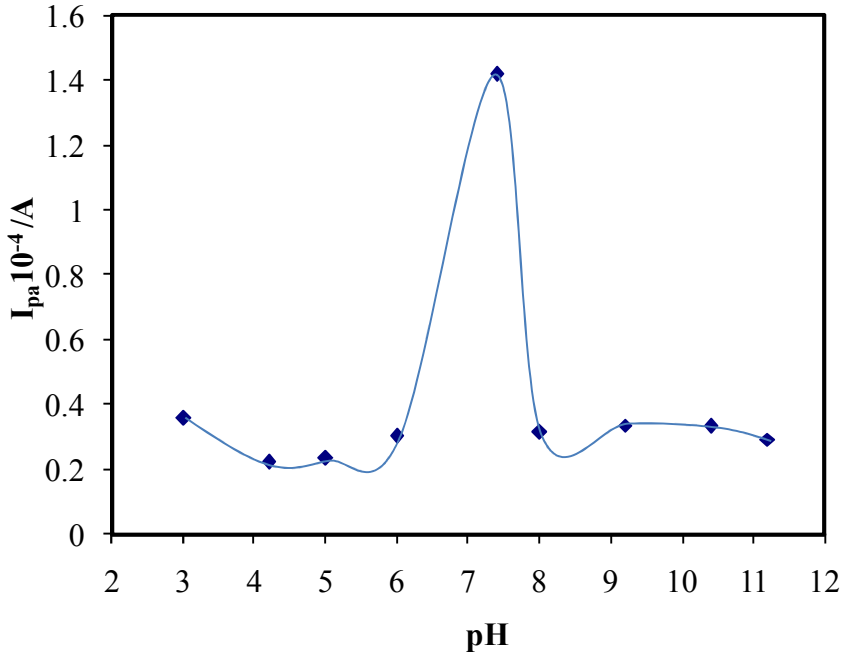

**Fig. 4(a)**. Cyclic voltammograms of 1.0 $\times 10^{-4}$ M PCM on MWCNT-CTAB/GCE with different scan rates; (a) - (p), 25 - 400/mV $s^{-1}$, in phosphate buffer with pH 7.4.

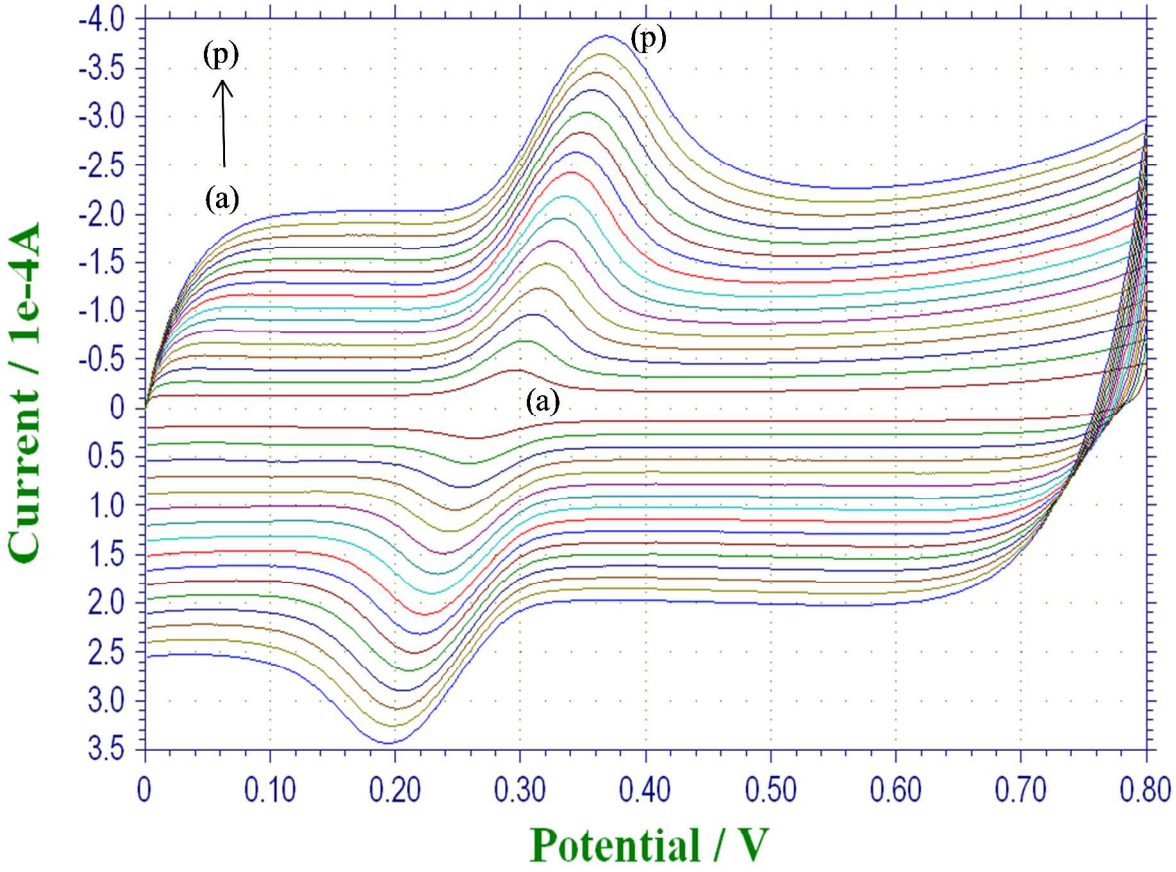


**Fig. 4 (b)**. Relationship between anodic and cathodic peak current vs. scan rate.

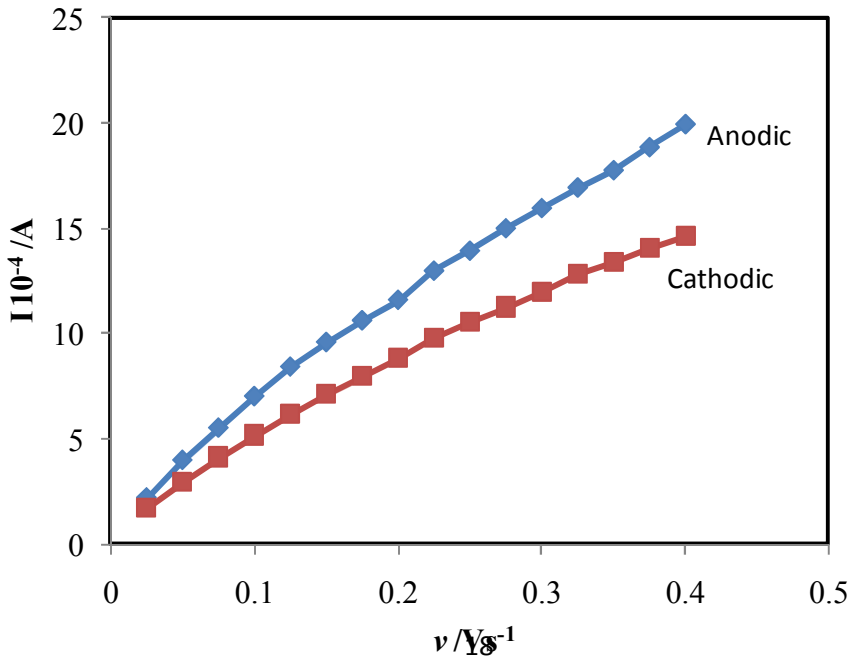

**Fig. 4(c)**. Relationship between anodic and cathodic peak potential vs. log of scan rate.

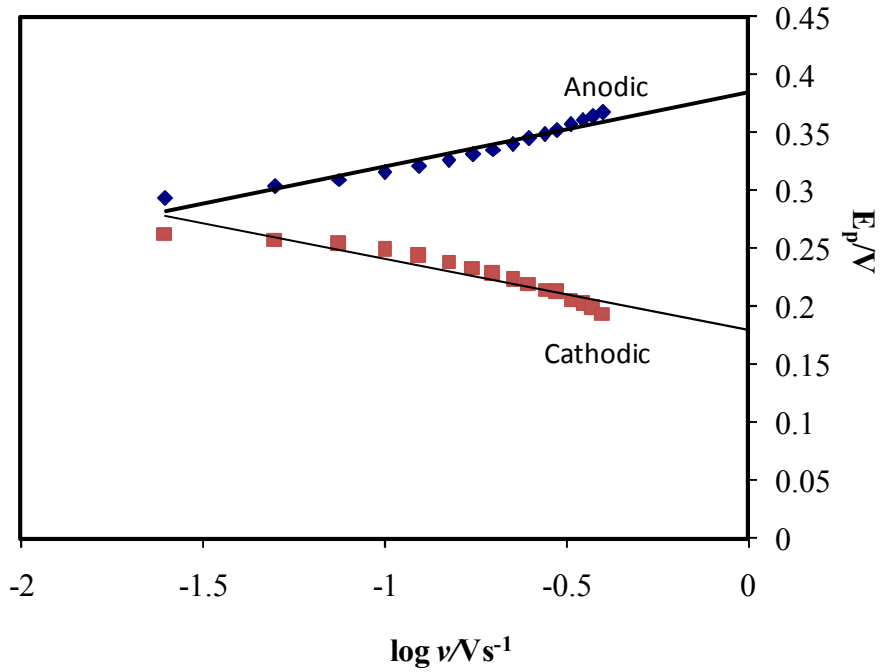


**Fig. 5.** UV-visible spectra of electrolyzed solution. (a) before electrolysis, (b) after electrolysis.

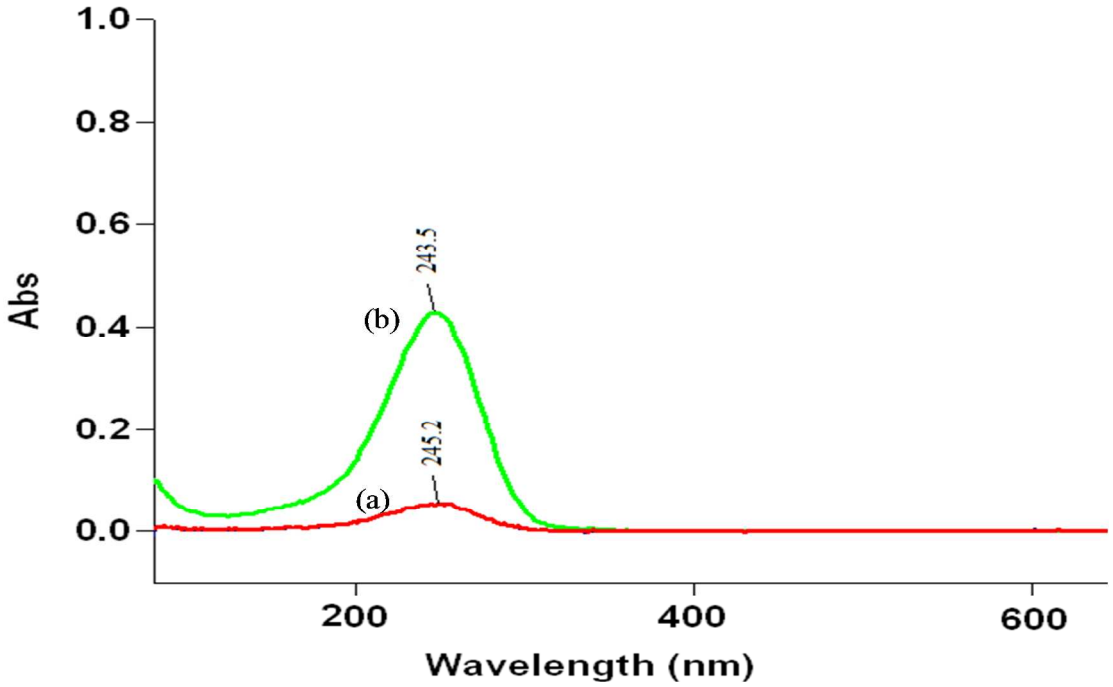

**Fig. 6(a)**. DPV curves of different concentrations of PCM (1-17: $4.0 \times 10^{-7}$ M - $4.0 \times 10^{-6}$ M) in 0.2 M pH 7.4 phosphate buffer solution.

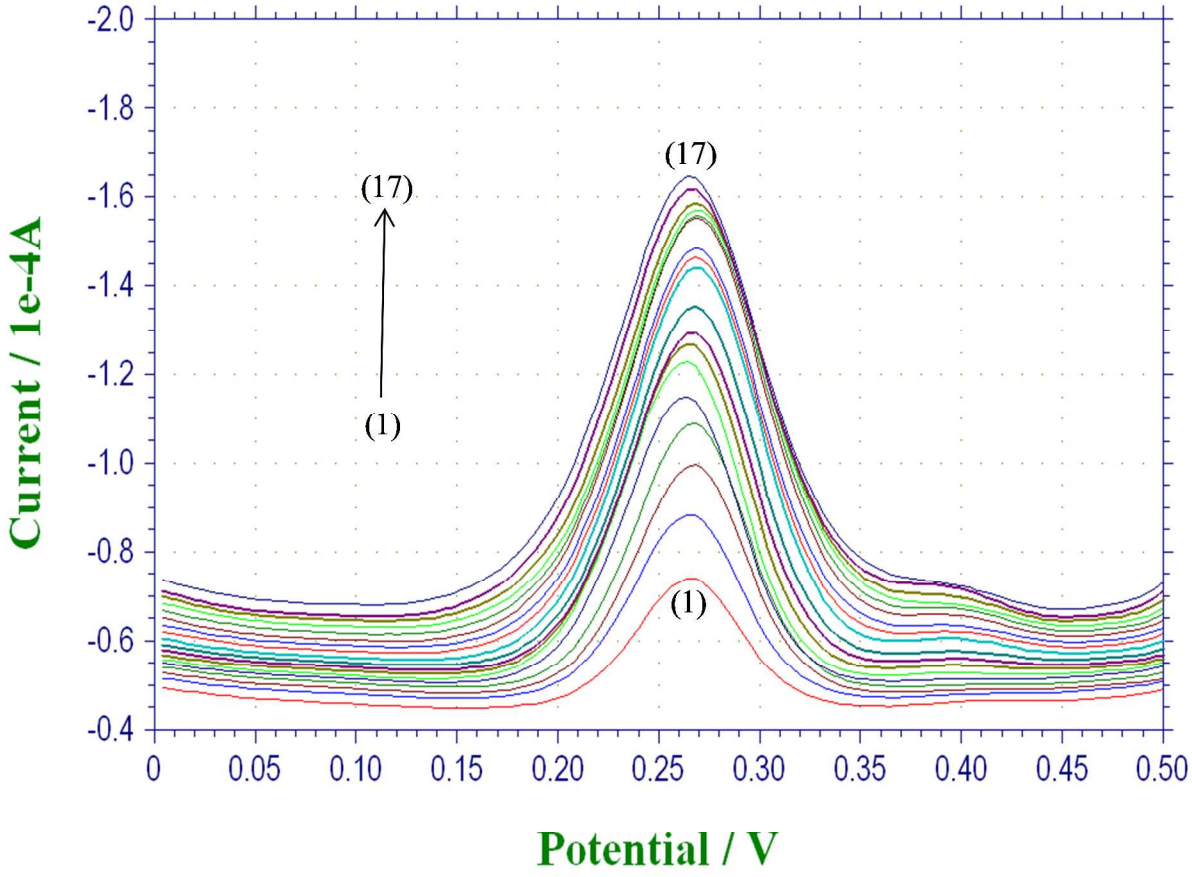


**Fig. 6(b).** Plot of peak current $I_{pa}$ against concentration of PCM (μM).

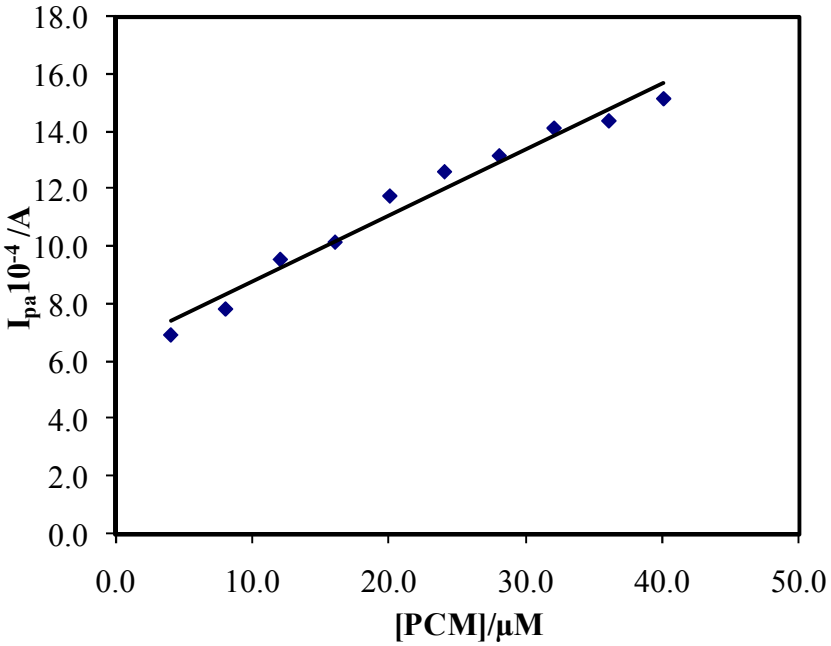

**Fig. 7(a).** Overlay spectrum of paracetamol showing various spectra at different concentration of drug(1)-(8): 2 µM to 150 µM.

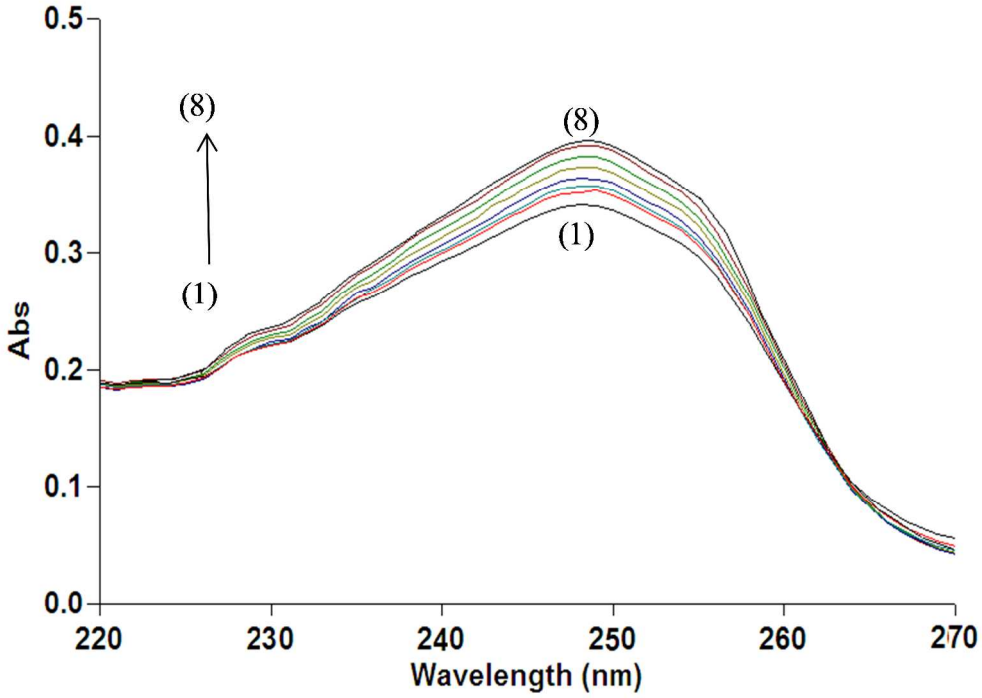


**Fig. 7(b).** Calibration curve of paracetamol in phosphate buffer solution of pH 7.4 at λ max 248 nm.

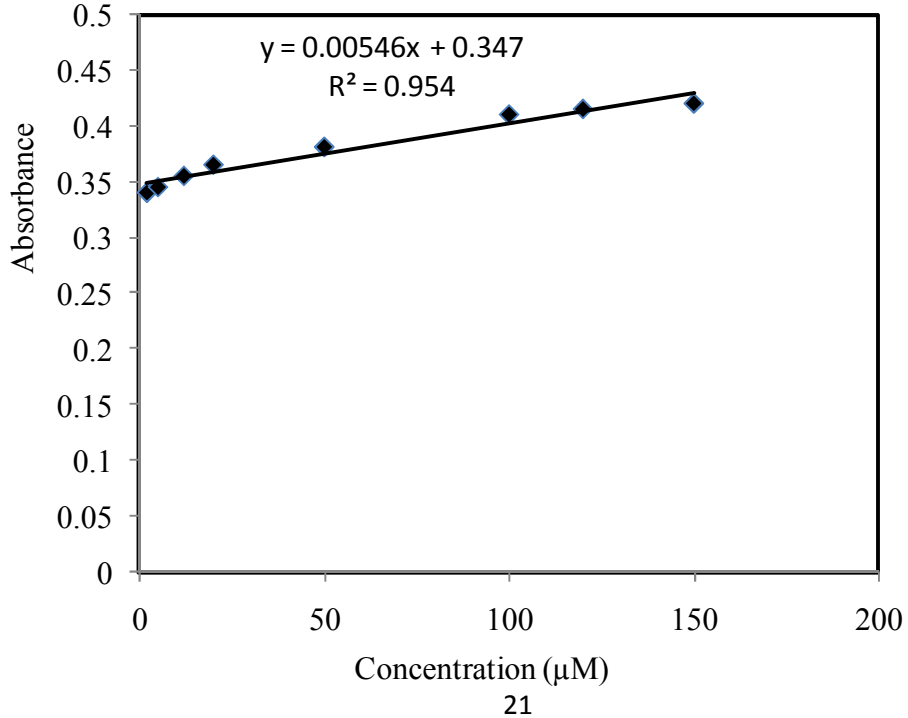

**Scheme 1.** Probable electro-oxidation mechanism of PCM.

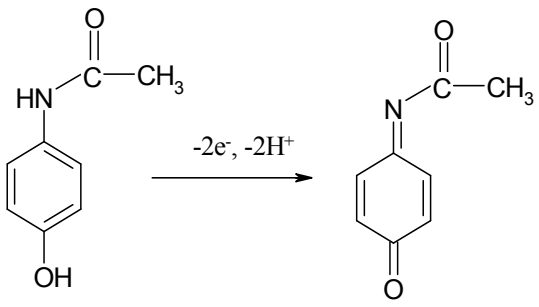

**Table 1.** Characteristics of PCM calibration plot using differential pulse voltammetry and UV-vis spectroscopy at MWCNT-CTAB modified GCE.

| | DPV method | UV-vis method |
|---|---|---|
| Linearity range | $4.0\times10^{-7}$ M to $4.0\times10^{-6}$ | $2.0\times10^{-6}$ M to $15.0\times10^{-5}$ |
| Slope of the calibration plot | 2.444 ±0.00044 | 0.00546±0.00067 |
| Intercept | 6.496±0.0062 | 0.3475±0.0001 |
| Correlation coefficient(r) | 0.972 | 0.954 |
| RSD of slope (%) | 1.609 | 1.116 |
| RSD of intercept (%) | 0.869 | 0.437 |
| Number of data points | 10 | 08 |
| LOD (M) | $4.82\times10^{-9}$ M | $3.39\times10^{-6}$ M |
| LOQ(M) | $1.60\times10^{-8}$ | $1.13\times10^{-5}$ M |
| Reproducibility of the electrode(%) | 2.5 | |
| Repeatability of the electrode(%) | 3.0 | |

**Table 2**. Summary of sensors reported by other authors for paracetamol detection using CNT-electrodes.

| Electrode | Linear range(μM) | LOD | Reference |
|---|---|---|---|
| 1. single-walled carbon nanotube-modified carbon–ceramic electrode | 0.2–150 | 0.2 | 29 |
| 2. SWCNT-Graphene Sheet modified GCE | 0.05–64.5 | 0.038 | 30 |
| 3. MWCNT/GCE | 26–340 | 0.029 | 31 |
| 4.MWCNT-carboxylic acid/GCE | 0.5–100 | 0.42 | 32 |
| 5. MWCNT-carboxylic acid/GCE | 0.074–230 | 0.040 | 33 |
| 6.MWCNT-polyhistidine/GCE | 0.25–5 | 0.032 | 34 |
| 7. MWCNT-chitosan/GCE | 2–250 | 0.16 | 35 |
| 8. PDDA-PSS/GPE | 25–400 | 0.5 | 36 |
| 9. DHPB/CNTP | 15.0–270 | 10 | 37 |
| 10. DMBQ/CNTP | 3.0–600 | 0.9 | 38 |
| 11.DHCA/CNTP | 2.0–400 | 0.8 | 39 |
| 12. CPB/CNTP | 39.4-136 | 2.1 | 40 |
| 13. BDDE | 0.01-0.1 | 0.85 | 41 |
| 14. Redox polymer MWCN | 0.25–1.50 | 1.0 | 42 |
| 15. Carbon-coated Ni nanoparticles | 7.80–110 | 2.30 | 43 |
| 16.Nefion@/Ru oxide | 5–250 | 1.20 | 44 |
| 17. MWCNT-CTAB/GCE | 0.4-4.0 | 0.00482 | **Present Work** |

PSS: poly styrene sulfonate, PDDA: poly (diallyldimetheylammonium chloride), DHPB: N-(3,4-dihydroxyphenethyl)-3,5-dinitrobenzamide, DMBQ: 8,9-dihydroxy-7-methyl-12H-benzothiazolo[2,3-b]quinazolin-12-one, DHCA: 3,4-dihydroxycinnamic acid; CPB: cetylpyridinium bromide, BDDE: Boron doped diamond electrode, CNTP: Carbon nanotube paste.

**Table 3**. Results of the assay and the recovery test of PCM in pharmaceutical preparations using DPV.

| | PYREMOL 650 |
|---|---|
| Labeled claim (mg) | 650 |
| Amount found (mg)[a] | 641.4 |
| Recovery (%) | 98.67 |
| RSD (%) | 0.38 |
| Bias (%) | 1.32 |
| Amount of pure drug added (mg) | 2 |
| Amount found (mg)[a] | 1.979 |
| Recovery (%) | 98.95 |
| RSD (%) | 1.05 |

[a] Average of five determinations

**Table 4.** Influence of potential excipients on the voltammetric response of $1.0 \times 10^{-6}$ M PCM.

| Excipients(1.0 mM) + Drug ($1.0 \times 10^{-6}$) | Potential observed (V) | Signal change (%) |
|---|---|---|
| Only paracetamol | 0.255 | 0 |
| Citric acid + PCM | 0.264 | 3.52 |
| Dextrose + PCM | 0.252 | -1.17 |
| Glucose + PCM | 0.245 | -3.92 |
| Gum acacia + PCM | 0.184 | **-27.84** |
| Tartaric acid + PCM | 0.262 | 2.74 |
| Starch + PCM | 0.252 | -1.17 |
| Oxalic acid + PCM | 0.267 | 4.7 |

**Table 5**. Determination of PCM in human plasma and urine samples.

| Sample | Spiked ($10^{-6}$ M) | Found[a] ($10^{-6}$ M) | Recovery (%) | RSD(%) |
|---|---|---|---|---|
| Urine Sample 1 | 1.0 | 0.979 | 97.9 | 0.085 |
| Urine Sample 2 | 5.0 | 4.96 | 99.2 | 0.044 |
| Plasma Sample 1 | 3.0 | 2.921 | 97.36 | 0.087 |
| Plasma Sample 2 | 8.0 | 8.104 | 101.3 | 0.014 |

[a] Average of five determinations